Geometrical Modelling Effects on FEA of Colorectal Surgery

Robinson Guachi[1], Michele Bici[2], Lorena Guachi[3], Francesca Campana[4], Fabiano Bini[5] and Franco Marinozzi[6]

[1]Sapienza University of Rome, robinson.guachi@uniroma1.it
[2]Sapienza University of Rome, michele.bici@uniroma1.it
[3] Yachay Tech University, lguachi@yachaytech.edu.ec
[4]Sapienza University of Rome, francesca.campana@uniroma1.it
[5]Sapienza University of Rome, fabiano.bini@uniroma1.it
[6]Sapienza University of Rome, franco.marinozzi@uniroma1.it

Corresponding author: Robinson Guachi, robinson.guachi@uniroma1.it

ABSTRACT

The research reported in this paper applies an explicit non-linear FEA solver to simulate the interaction between a clamp and a hyper-elastic material that aims to mimic the biological tissue of the colon. More in detail, the paper provides new results as a continuation of a previous works aimed at the evaluation of this solver to manage contact and dynamic loading on complex, multiple shapes. Results concern with the evaluation of the contact force during clamping, thus to the assessment of the force-feedback.
The analysis is carried out on two geometries, using the hyper-elastic Mooney-Rivlin model for the mechanical behavior of the soft tissues. A pressure is applied on the colon to simulate the surgical clamp, which goes progressively in contact with tissue surface. To assess FEA criticality, and, then, its feasibility, the stress-strain and the contact force are analysed according to geometrical model and thickness variation, leaving the pressure constant. Doing so, their effect on the force-feedback can be foreseen, understanding their role on the accuracy of the final result.

Keywords: Finite element analysis, soft tissues simulations, computer assisted surgical planning, segmentation.
DOI: https://doi.org/10.14733/cadaps.2019.778-788

1 INTRODUCTION

The development of new technologies and advances in computational efficiency have improved the linkage between different fields of science, as, for example, mechanics and medicine. Recently, Finite Element Analysis (FEA) has increased its applications in medical field, with the aim of design and improve prosthesis, orthosis and implants, [1],[2],[24], giving also the possibility of making preoperative plans and surgery simulations. [13].

In recent years, on the other hand, Minimally Invasive Surgery (MIS) has increased its applications, either using surgical assistant robot or following traditional (manual) way [17]. Nevertheless, in parallel to this increase of application fields, new issues also arise. In particular, instruments must be inserted through a trocar to access the abdominal cavity, without capability of direct manipulation of tissues, so that a loss of sensitivity occurs. This loss is caused by the absence of a direct force-feedback, resulting from the interaction between surgical instruments and soft tissues. While performing surgeries of a high level of complexity, through robots or trocar-guided instruments, filling this lack represents a great challenge.

More in detail, the lack of force-feedback represents a problem in several areas, which are strongly linked to engineering simulations, as, for instance:

- **PREOPERATIVE PLANNING.** The insertion of instruments, during surgery, causes deformations not only on target and surrounding tissues, but also on instruments themselves. The knowledge of force-feedback can help, during preoperative phase, in order to let the instrument able to reach the specific target areas, planning its line of action and displacements. In addition, it is possible to protect instruments and organs from damage, optimizing lines of action preventively.
- **SURGICAL SIMULATORS AND TELEOPERATION.** The complexity and wider diffusion of MIS require skilled and trained operators. For this reason, surgical simulators have been developed in order to accelerate the learning curve. Currently, these surgical simulators report feedback principally in terms of visual output, with a lack of haptic information about the forces. This is also due to the fact that a simulation of the real behavior of soft tissues may request high computational resources. The analysis of contact forces through simulation can avoid damages to tissues, improving skills. Analogous issues arise with teleoperation systems.
- **SURGICAL ROBOT ASSISTANT.** Principally, a robot can allow the usage of instruments with reduced dimensions, giving the possibility to reduce the number of access points. This is one of the fundamental aspects of MIS [17], allowing faster recover for the patient. In addition, through a robot, the natural vibrations of the operator hands can be avoided. Last but not least, a robot assistant can make a surgery safer, through the use of virtual fixtures, in order to avoid possible wrong movements, accidentally made by the surgeon. Currently, the usage of virtual fixtures involves significant physical constraints on the instrument. The increase of force-feedback accuracy can lead to an optimized usage of the virtual fixtures (improving safety, accuracy and speed of the robotized tools) [16].

As explained, FEA tools may increase the understanding of phenomena present in surgery when they are used to elaborate preoperative plans and to improve surgical procedures. Therefore, FEA may take an important role, to understand the distribution of stress-strain and the contact force instrument-tissue.

To get useful results using FEA, it is mandatory to take into account: (a) the mechanical behavior of tissues, and (b) the geometrical model and boundary conditions of the anatomical district. Many problems are connected to both of these steps and all of them affect results accuracy. In our research, we focused on colorectal tissues simulations, in order to understand the present effects during the interaction between surgical instruments and soft tissues in terms of stress-strain distribution, as well as the contact force that is produced on the instrument.

In [12], we started the analysis of these topics, according to different constitutive material models for the mechanical behavior of the tissue and to different complexities of the geometric model. In particular, it confirms that a Linear Elastic mechanical behavior does not reproduce a real stress-strain distributions related to large displacement, while a hyper-elastic does. Having in mind the necessity of computations that could be not dramatically expensive and easy to be provided, we tested a hyper-elastic material model (Mooney-Rivlin). It is already implemented in a commercial code, RADIOSS, and it is rather easy to be fit with experimental data, since only two material constants have to be provided (under the hypotheses of uncompressible volume). This solver is an explicit code [26] for highly non-linear problems (due to large displacements and/or plastic behavior) under dynamic loadings. It is currently adopted for crashworthiness analyses, which involves many contact conditions, among different parts or in self-contacts, or virtual set-up of manufacturing processes with high non-linearity due to the material. These prerogatives convinced us to investigate its feasibility for the set-up of a FEA evaluation of force-feedback on the clamp. In fact, in our case, there are: (a) contact with a tissue characterized by non-linear behavior, (b) kinematic paths that involve contact with other tissues and, more in general, dynamic loads.

In this paper, we are going to present an extension of this work, investigating how geometrical changes of the organ will affect contact force and strain-stress distributions. More in detail, we are going to correlate the results of stress, strain and contact force on the clamp, changing the accuracy of the organ's shape and the initial thickness of its wall (assumed as constant). In Section 2, we introduce the state of the art concerning digitalization of geometry, FEA in soft tissues and related investigation about material models. Section 3 explains our specific case-study, while Section 4 presents the achieved results and, finally, in Section 5, we highlight conclusions and guidelines for future works.

2 METHODS

As already reported in the introduction, for non-linear problems, accuracy of a FEA is strongly related to the accuracy of the part geometry and the constitutive material used to describe the mechanical behavior of the tissue.

Accurate geometrical models can be derived from acquisition through Data Imaging and Communications in Medicine (DICOM). Doing so, FEA may become a useful virtual-prototyping tool, which is able to take into account the particular characteristics of each patient that will undergo surgery [13]. Nevertheless, simplified models may be used [18] for validations of FEA according to simplified experiments or to new material models.

2.1 Digitalization of geometry

To perform the geometry digitalization, it is necessary to segment the images. Image segmentation is a technique that deals with separating input data into meaningful parts of the images, with their respective borderlines, which represent different objects. It is aimed on the increase of the quality of data and information present in a 2D image, isolating areas of interest (operatively, this process can be seen as a reduction of misclassified pixel in the image) [8].

Medicine is a constantly expanding field that also applies medical image segmentation in several imaging and acquisition modalities (MRI, Computed Tomography (CT) [25], Positron Emission Tomography (PET), X-RAY, and Ultrasound). Medical image segmentation identifies and isolates areas of interest in input data in order to analyze the geometrical model of a tissue or an organ. It splits up the input data into organs and tissues regions using features such as colors, texture, motion and edges among others. However, the automatic segmentation is still a challenge, due to the presence of added noise, artefacts, limitations, and unclear edges [14].

According to [19], a precise and automatic segmentation of colon from images is a challenging problem of many clinical applications in colonography, including, for example, computer-aided detection of colon polyps and 3D virtual flythrough of the colon. Automatic segmentation step [14] provides computational models diminishing the time-consumption and laborious manual process. The manual process usually demands a lot of time to identify and draw borderlines around tissues present in a single tomographic image. The issue is magnified because of the large number (300–600) of images that are required to span the head-to-foot anatomy of an individual through steps of about 3 mm. For this reason, in the recent past, semi-automatic and automatic segmentation have been extensively subject of research efforts [5],[11].

2.2 Mechanical properties

To develop a finite element analysis in a customized way, each FE simulation should require specific mechanical properties of the patient's tissues. These mechanical properties should be measured "in vivo", but this requirement demands a non-destructive method of material characterization. Unfortunately, the existing probes provide qualitative rather than quantitative information, since each tissue is connected by fasciae [18]. For this reason, most of the mechanical properties are measured "ex vivo" using destructive in vitro mechanical tests. Ideally, with a high number of cases and samples available, it could be possible to obtain standard values for material characterization, depending on gender, age, tissue typology, previously encountered pathologies, etc.. Nevertheless, even today, really few tests can be found in literature because it is difficult to characterize the mechanical behavior of tissues, also in "ex-vivo" tests. However, many laboratory tests [7],[15],[20],[21] have been performed to determine the mechanical properties of soft tissues both in people and in animals. Generally speaking, soft tissues have a hyper-elastic behavior, as highlighted in [21].

Several FEA works have used different models of mechanical behavior (linear elastic or hyper-elastic), trying to reproduce the real behavior of soft tissues [6],[13].

The model to be used depends on the goal of the simulation. In fact, in case of simulations oriented to train new surgeons through virtual reality, a decrease of the computational cost for simulating in real time may ask for a linear elastic model. The Hyper-elastic models [6],[13],[18], are necessary when major accuracy is requested in the stress-strain evaluation, like in preoperative planning (tissue detachment, implant analysis, etc.), admitting the higher time consumption.

In the hyper-elastic field, the most suitable models to reproduce soft tissue behavior are two hyper-elastic models: Mooney-Rivlin model and Yeoh model. They are phenomenological material models used in FEA [12] to perform non-linear analysis in materials as rubber [22].

Usually, hyper-elastic models are described by the stored energy, in the unit of reference volume of the material (W). The Mooney-Rivlin model [23] is described through the first and second invariants of the Green deformation tensor (I_1, I_2), while the YEOH model [23] is described only through the first invariants of the Green deformation tensor.

For the Mooney-Rivlin model:

$$W = C_{10}(I_1 - 3) + C_{01}(I_2 - 3) + \frac{1}{D_1}(J_{el} - 1)^2 \tag{2.1}$$

Considering the tissue as uncompressible, the equation becomes

$$\mathrm{W} = \mathrm{C}_{10}(\mathrm{I}_1 - 3) + \mathrm{C}_{01}(\mathrm{I}_2 - 3) \tag{2.2}$$

For what concerns Yeoh model:

$$W = \sum_{i=1}^{3} C_{i0}(I_1 - 3)^i + \sum_{i=1}^{3} \frac{1}{D_i}(J_{el} - 1)^{2i} \tag{2.3}$$

Considering the tissue as uncompressible, the equation becomes

$$W = \sum_{i=1}^{3} C_{i0}(I_1 - 3)^i \tag{2.4}$$

Where W represents the stored energy density function, J_{el} stands for Elastic volume ratio; C_{10}, C_{01}, C_{i0} are constants characteristics of the material and D_1 is material constant that control bulk compressibility.

3 CASE STUDY AND MODELLING

The case study investigated through FEA is the interaction between a surgical clamp and part of the colorectal tissue, to analyze stress, strain and contact force, when a variation of the tissue thickness occurs, evaluating the sensitivity to this parameter. The case study has been analyzed in each of the different geometrical models. In Fig. 1, we can see the area of interest in red.

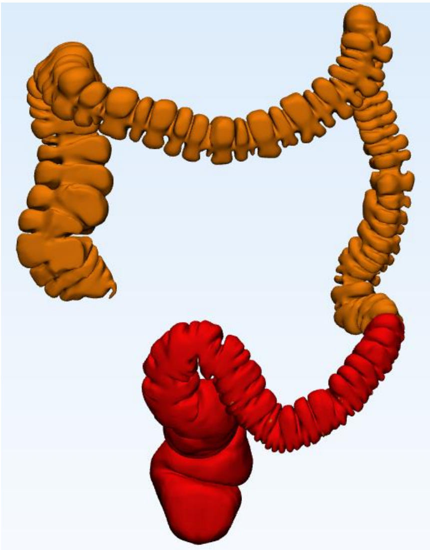

Figure 1: Virtual model of large intestine (Colon).

3.1 Geometrical modelling of the surfaces

Geometrical models studied in this paper represent a part of the entire colon, placed in the zone between the sigmoid area and the rectum area, as reported, in red, in Fig. 1. We consider two different geometrical models:

- **Cylindrical Surface (CS).** It represents a simplified, symmetric and uniform geometry. It is an idealization of the colorectal tissue shape, modelled with an outer diameter of 25mm and a length of 100 mm, with the grasp positioned in the middle section of the cylinder, Fig. 2(a).
- **MRI Surface (MRI).** It represents a geometrical model obtained from the segmentation of MRI (Magnetic Resonance Imaging) images, Fig. 2(b). MRI images were acquired by means a 1.5 T scanner (Sonata Siemens, Erlangen, Germany), with a phased-array body surface coil.

In cases of MRI model, a semi-automatic segmentation was performed by means of Slicer3D (Version 4.5) [10], according to DICOM procedures. Generally, manual operations may increase local accuracy but they are complex to be checked and replicated on a large number of slices. Nevertheless, they are a valid option in cases of limited parts of organs or small details, as in the considered case. The assumption of avoiding the consideration of circular folds is due to the goal of reduction of time consumption maintaining a complex surface, close to the real shape, without local folds that can increase the computation time, adding no significant accuracy.

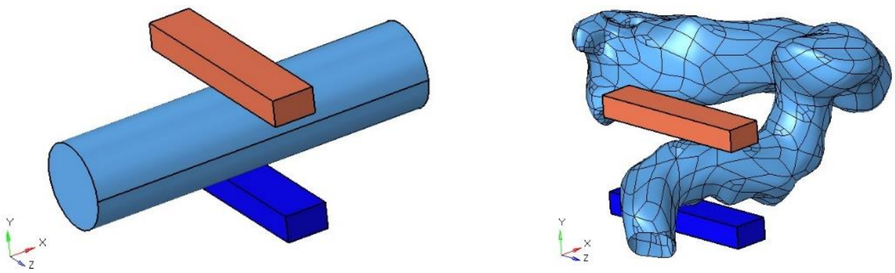

(a) (b)

Figure 2: Geometrical models: (a) Circular Surface (CS), and (b) MRI Surface (MRI).

After the segmentation, it was necessary to perform a post-processing of the geometrical model achieved by MRI, in order to check and optimize it. Then, the model was imported into a CAD software for Reverse Engineering process [4]. The optimization process started from the STL tessellation of the 3D model adopting Reverse Engineering techniques for free-form modelling. Additionally, it is necessary to merge shells that conform the colon tissues, to manually isolate and delete the outliers, performing also holes recovery, if necessary.

The adoption of two geometrical models is made according to some authors that recommend to study a simplified geometry, as uniform and symmetrical as possible, to understand the physical behavior in a general way [18]. Then, this understanding can be used to evaluate results of increasingly realistic cases, arriving up to the real patient case. In our case, FEA related to CS may help to understand the distribution of stress-strain without taking into account particular geometrical irregularities which are present in MRI. In particular, as shown in Fig. 3, the MRI has many local changes in the diametrical length of section.

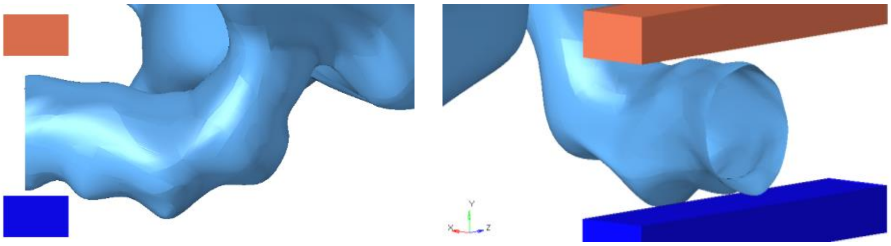

(a) (b)

Figure 3: MRI surface: Changes in the diametrical length of section.

3.2 FEA set-up

In this paper, the analysis is carried out on two geometries, showed in Fig. 2, as surface models, and in Fig. 4, as FEA meshes. They are modeled with triangular shell elements (as provided through Delaunay's tessellation). Elements are of the first order with mesh-quality values suitable for FEA: the max length is 5.66 mm, the maximum skew angle is equal to 77°, the minimum jacobian is 1, Equia skew is 0.6. For each geometrical model, we assumed initial thickness as constant in each element of the mesh. Since one of the goals of the paper is the understanding of effects of initial thickness on stress and strain results, we have considered thickness variations from 0.8 mm to 2 mm, as founded in literature [9],[15],[18],[20].

Fig. 4 shows the meshes. In [12], it is possible to observe a convergence of results using a mesh length of 2mm. To decrease the computational cost, a discretization using a 2 mm mesh-length has been carried out in the area subjected to the contact and nearby. Outside these areas, a larger mesh with length up to 5.66 mm has been provided.

For the mechanical behavior, we have selected the Mooney-Rivlin hyper-elastic model [23], assigning to C_{10} and C_{01} the values of 0.083MPa and 0.0565MPa respectively, as reported in [12].

The two geometrical models have been considered related to an empty colon, as reported in Fig. 4, because patients generally have to comply with a pre-operative plan for emptying digestive system before the surgical operation.

The surgical clamp has been discretized by hexahedral elements. In this case, the fasciae between organs are not considered. Initial condition of the clamp is open without contact, as shown in Fig. 2. Surgical clamp has been assumed as a rigid body (represented though the blue and brown volumes of Fig. 2, Fig. 3 and Fig. 4).

The load on the clamp, during its closing, has been chosen consistent with the recommended pressure experimented for closing completely the section of the colon, 8 gr/mm^2 [3]. This value represents the pressure exerted on the surgical clamp to guarantee, at the end of its motion along the "Y" direction, the self-contact of the tissues and, also, the grasping of tissues between the two sides of the clamp. In our case, the pressure is directly applied at the top of the surgical clamp (upper side of the brown part of the clamp in Fig. 4) along the "Y" direction.

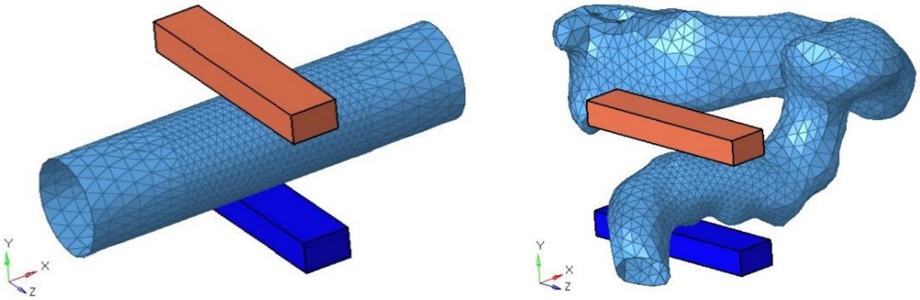

(a) (b)

Figure 4: Geometrical models: (a) Discretized CS Model, and (b) Discretized MRI Model.

Concerning boundary conditions, constraints; similar to real behavior, are difficult to be defined. In our case, the boundary conditions have been performed, simplifying, at the ends of the geometries, releasing rotations in all axes and displacements along colon axial direction (in the MRI case, the direction along which the displacements are released is parallel to the local center line, orthogonal to the cutting plane). This procedure is suitable to recreate constraints similar to conditions present in the tissue while performing colorectal surgery, assuming that the presence of the constraints at the ending sections do not interact with the results.

FEA simulations correspond to explicit non-linear dynamic analyses carried out in Hyperworks, using the RADIOSS solver. Contact and auto-contact conditions are provided according to the standard algorithms of the solver.

4 NUMERICAL RESULTS

In this section, we analyze the influence of thickness changes on the two FEA models (CS and MRI). Results are discussed according to the achieved stress-strain distributions, contact force and pressure.

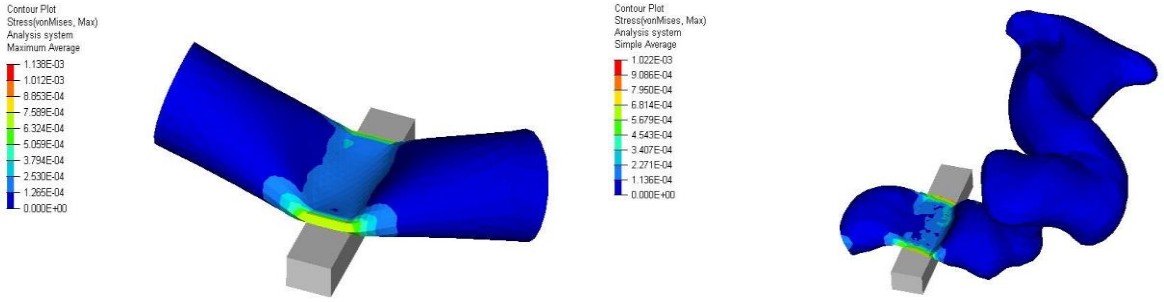

(a) (b)

Figure 5: Stress Contour-Maps (GPa) at the moment of maximum clamp tightening: (a) Stress Contour-Map in the CS Geometrical model, and (b) Stress Contour-Map in the MRI Geometrical model, the represented models are considered with 2mm. of thickness.

Fig. 5 shows the maximum equivalent stress distribution of the two geometrical models assuming an initial thickness of 2 mm. Both of them have stress concentration around the folds induced by the closing of the clamp, with similar ranges of values.

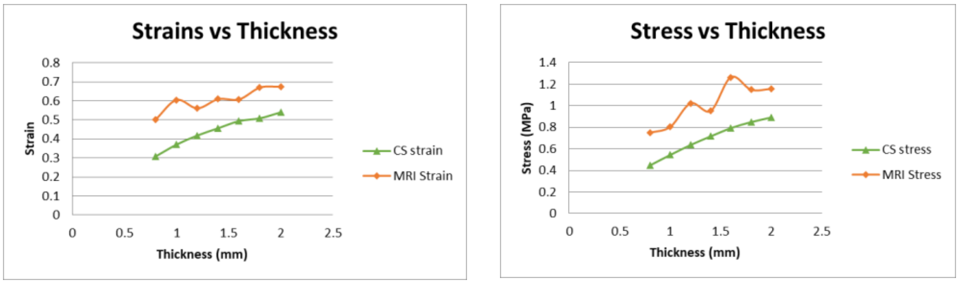

(a) (b)

Figure 6: Stress-Strain Curves: (a) Strain Vs Thickness, and (b) Stress Vs Thickness.

Fig. 6 highlights the comparison among strain and stress changing geometrical model and initial thickness. They are referred to the maximum values of the equivalent von Mises' stress that obviously occur in the areas of stress/strain concentration shown in Fig. 5.

Concerning changes in thickness, both geometrical models show an increase, although the MRI has irregular trends. This can be seen as an effect of the local changes in the diametrical sections of the MRI, as also shown in Fig.5 (b), in the flat area in contact with the upper part of the clamp. Effectively, in MRI during clamp motion, the contact between tissues and clamp is not regularly distributed, involving only several portions of surfaces. As a consequence, irregular distribution of areas in contact causes an irregular distribution of stress (and, thus, strain), as shown in Fig. 5(b).

The increasing trend of Fig. 6 is an obvious consequence of the increasing of the initial thickness. In fact, a higher thickness means a higher volume, with the possibility of absorbing a higher level of energy, locally converted into stress and strain. In addition, the increasing trend may be also partially connected to the fact that the FEA condition has an imposed motion on the clamp that is stopped at a specific gap-value related to clamp tighten. This means a maximum limit for the distance between clamps, but, with an increase of the initial thickness, it leads to higher stresses in the tissue that is more compressed.

Despite the presence of an irregular trend of stress and strain, the MRI increment of the stress and the strain according to the range of the initial thickness is of 52% for the stress and 36% for the strain. CS shows higher values (115% and 80%, respectively). As already explained in [12], it can be correlated to the local irregularities of the MRI that involve the large displacement hypotheses more intensively than CS.

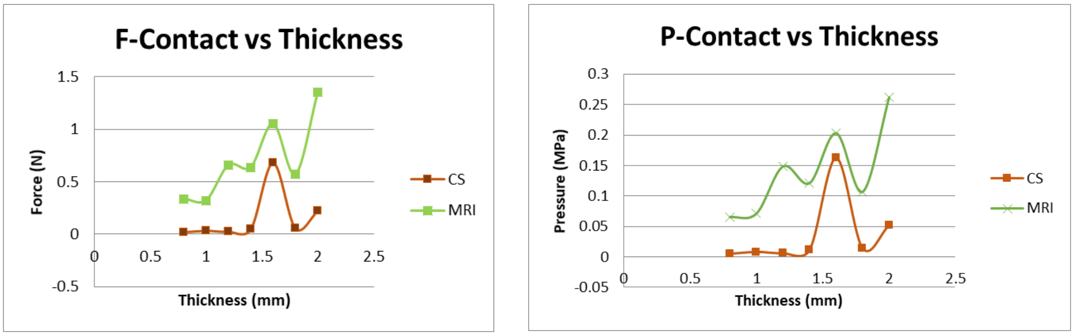

(a) (b)

Figure 7: Force and Pressure Curves: (a) Force Vs Thickness, and (b) Pressure Vs Thickness.

Fig. 7 shows interaction analysis between geometrical model and thickness change on contact force between clamp and tissue (it is a reaction force of the tissue upon the clamp) and the correlated pressure. CS seems to produce a rather constant reaction force, despite the peak at 1.8 mm of initial thickness. Oscillations of the MRI model can be again explained as a geometrical effect. It can be said that a more irregular surface involves a higher reaction, so a higher contact force. In addition, an irregular surface, like MRI, causes that only several zones, during clamping, are in contact. This leads to an increase in terms of pressure. Otherwise, concerning Fig. 7, major investigation are necessary due to the unexplained results of CS.

5 CONCLUSIONS

The paper provides new results related to the application of an explicit FEA solver, RADIOSS, to analyze the interaction between a clamp and a colorectal tissue, based on the Mooney-Rivlin constitutive model. Advantages of its adoption are:

- Reliable contact algorithms for non-linear applications also under dynamic loads (e.g. during clamp movement in the organ district) with relative low consumption of computational resources;
- A constitutive model based only on two constants, to be evaluated from experimental data.

The two evaluated geometrical models (CS and MRI) help to understand how changes, related to shape complexity, influence the stress-strain results. The soundness of these results, although not validated yet, confirms again the feasibility of this kind of solver, in this field.

They confirm that passing from CS to MRI, geometrical non linearity becomes more relevant, affecting the maximum values of stress, strain and forces. CS and MRI have similar trends according to the value of the initial thickness. An increase of initial thickness provides higher values of stress and strain, but it does not seems to be so effective for the reaction force in the case of CS. Major investigations are necessary.

Thickness changes, in the real tissues, may occur due to disease or inflammation. So, next developments should be the set of different areas of thickness inside a single case, also considering circular folds or polyps.

Both the simplified geometries (CS and MRI), used in this paper, may be useful for obtaining an evaluation of the force feedback, through the FEA, in order to manage reactions that, for example, can be seen as input for the cinematic chain of a haptic system., or for the optimization of the design of the instruments. In particular, CS can be useful for experimental validation, while FEA on MRI, with more detailed elements of the surface of the clamp, the colon folds, and so on, may provide contact forces for a preliminary tool for the assessment of force-feedback.

Robinson Guachi, http://orcid.org/0000-0002-0476-6973
Michele Bici, http://orcid.org/0000-0002-7744-2152
Lorena Guachi, http://orcid.org/0000-0002-8951-8150
Francesca Campana, http://orcid.org/0000-0002-6833-8505
Franco Marinozzi, http://orcid.org/0000-0002-4872-2980

REFERENCES

[1] Araneo, R.; Rinaldi, A.; Notargiacomo, A.; Bini, F.; Pea, M.; Celozzi, S.; Marinozzi, F.; Lovat, G.: Design concepts, fabrication and advanced characterization methods of innovative piezoelectric sensors based on ZnO nanowires, Sensors, 14(12), 2014, 23539-23562. https://doi.org/10.3390/s141223539
[2] Araneo, R.; Rinaldi, A.; Notargiacomo, A.; Bini, F.; Pea, M.; Celozzi, S.; Marinozzi, F.; Lovat, G.: Effect of the scaling of the mechanical properties on the performances of ZnO piezo-semiconductive nanowires, AIP Conference Proceedings, 1603, 2014, 14-22. https://doi.org/10.1063/1.4883037
[3] Baker, R-S.; Foote, J.; Kemmeter, P.; Brady, R.; Vroegop, T.; Serveld, M.: The science of stapling and leaks, Obesity surgery, 14(10), 2004, 1290-1298. https://doi.org/10.1381/0960892042583888
[4] Campbell, R-J.; Flynn, P-J.: A survey of free-form object representation and recognition techniques, Computer Vision and Image Understanding, 81(2), 2001, 166-210. https://doi.org/10.1006/cviu.2000.0889
[5] Caon, M.; Sedlář, J.; Bajger, M.; Lee, G.: Computer-assisted segmentation of CT images by statistical region merging for the production of voxel models of anatomy for CT dosimetry, Australasian Physical & Engineering Sciences in Medicine, 37(2), 2014, 393-403. https://doi.org/10.1007/s13246-014-0273-x
[6] Chen, Z-W.; Joli, P.; Feng, Z-Q.; Rahim, M.; Pirró, N.; Bellemare, M-E.: Female patient-specific finite element modeling of pelvic organ prolapse (POP), Journal of Biomechanics, 48(2), 2015, 238-245. https://doi.org/10.1016/j.jbiomech.2014.11.039
[7] Christensen, M-B.; Oberg, K.; Wolchok, J-C.: Tensile properties of the rectal and sigmoid colon: a comparative analysis of human and porcine tissue, SpringerPlus, 4(1), 2015, 142. https://doi.org/10.1186/s40064-015-0922-x
[8] Cocorullo, G.; Corsonello, P.; Frustaci, F.; Guachi, L.; Perri, S.; Multimodal background subtraction for high-performance embedded systems, Journal of Real-Time Image Processing, 2016, 1-17. https://doi.org/10.1007/s11554-016-0651-6
[9] Egorov, V-I.; Schastlivtsev, I-V.; Prut, E-V.; Baranov, A-O.; Turusov, R-A.: Mechanical properties of the human gastrointestinal tract, Journal of Biomechanics, 35(10), 2002, 1417-1425. https://doi.org/10.1016/S0021-9290(02)00084-2
[10] Fedorov, A.; Beichel, R.; Kalpathy-Cramer, J.; Finet, J.; Fillion-Robin, J-C.; Pujol, S.; Buatti, J.: 3D Slicer as an image computing platform for the Quantitative Imaging Network, Magnetic resonance imaging, 30(9), 2012, 1323-1341. https://doi.org/10.1016/j.mri.2012.05.001
[11] Gayathri, K.; Radhakrishnan, R.: Automatic Segmentation of Colon in 3D CT Images and Removal of Opacified Fluid Using Cascade Feed Forward Neural Network, Computational and Mathematical Methods in Medicine, 2015. https://doi.org/10.1155/2015/670739
[12] Guachi, R.; Bini, F.; Bici, M.; Campana, F.; Marinozzi, F.: Finite Element Model Set-up of Colorectal Tissue for Analyzing Surgical Scenarios, European Congress on Computational Methods in Applied Sciences and Engineering, Springer, Cham, 2017, 599-609. https://doi.org/10.1007/978-3-319-68195-5_65

[13] Jeanditgautier, E.; Mayeur, O.; Brieu, M.; Lamblin, G.; Rubod, C.; Cosson, M.: Mobility and stress analysis of different surgical simulations during a sacral colpopexy, using a finite element model of the pelvic system, International Urogynecology Journal, 27(6), 2016, 951-957. https://doi.org/10.1007/s00192-015-2917-0

[14] Kim, S.; Lim, H.: Method of background subtraction for medical image segmentation. Proceedings of the 3rd International Conference on Cybernetics and Information Technologies, Systems and Applications, 2006, 87-91.

[15] Liao, D.; Zhao, J.; Gregersen, H.: 3d Mechanical properties of the partially obstructed guinea pig small intestine. Journal of Biomechanics, 43(11), 2010, 2079-2086. https://doi.org/10.1016/j.jbiomech.2010.04.008

[16] Lopez, E.; Zollo, L.; Guglielmelli, E.: Teleoperated control based on virtual fixtures for a redundant surgical system, Intelligent Robots and Systems (IROS), 2013 IEEE/RSJ International Conference on IEEE, 2013, 450-455. https://doi.org/10.1109/IROS.2013.6696390

[17] Lorenzon, L.; Bini, F.; Balducci, G.; Ferri, M.; Salvi, P. F.; Marinozzi, F.: Laparoscopic versus robotic-assisted colectomy and rectal resection: a systematic review and meta-analysis, Int. J. Colorectal Dis., 2016, 31(2), 161-173. https://doi.org/10.1007/s00384-015-2394-4

[18] Mayeur, O.; Witz, J-F.; Lecomte, P.; Brieu, M.; Cosson, M.; Miller, K.: Influence of geometry and mechanical properties on the accuracy of patient-specific simulation of women pelvic floor. Annals of Biomedical Engineering, 44(1), 2016, 202-212. https://doi.org/10.1007/s10439-015-1401-9

[19] Navab, N.; Glocker, B.; Kutter, O.; Kirchhoff, S-M.; Reiser, M.: Medical Image Processing for Analysis of Colon Motility, Handbook of Biomedical Imaging, Springer US, 2015, 391-401. https://doi.org/10.1007/978-0-387-09749-7_21

[20] Qiao, Y.; Pan, E.; Chakravarthula, S-S.; Han, F.; Liang, J.; Gudlavalleti, S.: Measurement of mechanical properties of rectal wall, Journal of Materials Science: Materials in Medicine, 16(2), 2005, 183-188. https://doi.org/10.1007/s10856-005-5988-5

[21] Rubod, C.; Brieu, M.; Cosson, M.; Rivaux, G.; Clay, J-C.; de Landsheere, L.; Gabriel, B.: Biomechanical properties of human pelvic organs, Urology, 79(4), 2012, 968-e17. https://doi.org/10.1016/j.urology.2011.11.010

[22] Sasso, M.; Palmieri, G.; Chiappini, G.; Amodio, D.: Characterization of hyperelastic rubber-like materials by biaxial and uniaxial stretching tests based on optical methods, Polymer Testing, 27(8), 2008, 995-1004. https://doi.org/10.1016/j.polymertesting.2008.09.001

[23] Shahzad, M.; Kamran, A.; Siddiqui, M-Z.; Farhan, M.: Mechanical characterization and FE modelling of a hyperelastic material, Materials Research, 18(5), 2015, 918-924. https://doi.org/10.1590/1516-1439.320414

[24] Xu, K.; Goldman, R-E.; Ding, J.; Allen, P-K.; Fowler, D-L.; Simaan, N.: System design of an insertable robotic effector platform for single port access (SPA) surgery, Intelligent Robots and Systems, 2009. IROS 2009, IEEE/RSJ International Conference on IEEE, 2009, 5546-5552. https://doi.org/10.1109/iros.2009.5354028

[25] Yang, X.; Ye, X.; Slabaugh, G.: Multilabel region classification and semantic linking for colon segmentation in CT colonography, IEEE Transactions on Biomedical Engineering, 62(3), 2015, 948-959. https://doi.org/10.1109/TBME.2014.2374355

[26] Zienkiewicz, O.: The Finite Element Method, 1St Edn, McGraw-Hill, Maidenhead, (1977)